

Published in final edited form as:

*J Polym Sci A Polym Chem*. 2008 October 1; 46(19): 6630–6640. doi:10.1002/pola.22973.

## Introduction of pH-Sensitivity into Mechanically Strong Nanoclay Composite Hydrogels Based on *N*-Isopropylacrylamide

Siddhartha K. Mujumdar<sup>1</sup> and Ronald A. Siegel<sup>1,2,\*</sup>

<sup>1</sup> Department of Biomedical Engineering, University of Minnesota, Minneapolis, MN 55455, USA

<sup>2</sup> Department of Pharmaceutics, University of Minnesota, Minneapolis, MN 55455, USA

### Abstract

pH-sensitive nanoclay composite hydrogels based on *N*-isopropylacrylamide (NIPA) were synthesized by copolymerization with cationic and anionic comonomers. Laponite nanoclay particles served as multifunctional crosslinkers, producing hydrogels with exceptionally high mechanical strengths, as measured by elongation at break. Cationic copolymer gels based on NIPA and dimethylaminoethylmethacrylate were prepared by aqueous free radical polymerization, adopting a procedure reported by Haraguchi (*Adv Mater* 2002, 14, 1120–1124). Without modification, this technique failed to produce anionic copolymer gels of NIPA and methacrylic acid due to flocculation of clay particles. Three methods were conceived to incorporate acidic MAA into nanoclay hydrogels. First, NIPA was copolymerized with acidic comonomer under dilute conditions, producing hydrogels with good pH-sensitivity but weak mechanical characteristics. Second, NIPA was copolymerized with methyl methacrylate, which was then hydrolyzed to generate acid sidegroups, yielding hydrogels that were much stronger but less pH sensitive. Third, NIPA was copolymerized with an acid comonomer following modification of the nanoclay surface with pyrophosphate ions. The resulting hydrogels exhibited both strong pH-sensitivities at 37 °C and excellent tensile properties. Optical transparency changed during polymerization, depending on hydrophobicity of the components. This work increases the diversity and functionality of nanoclay hydrogels, which display certain mechanical advantages over conventionally crosslinked hydrogels.

### INTRODUCTION

Stimuli-sensitive hydrogels have been widely investigated for an extensive range of pharmaceutical and biomedical applications including drug delivery,<sup>1–3</sup> tissue engineering,<sup>4–6</sup> sensors<sup>7,8</sup> and soft actuators.<sup>9–11</sup> Depending on backbone structure and composition, such gels can be engineered to respond to external stimuli such as temperature, pH,<sup>12</sup> light<sup>13</sup> and electric field.<sup>14–15</sup> For example, hydrogels of *N*-isopropylacrylamide (NIPA) are swollen below 33 °C but shrink above that temperature, which is often called the lower critical temperature, or LCT. These hydrogels are rendered pH-sensitive by copolymerizing NIPA with acidic or basic comonomers, often at low degree of substitution. Changes in pH affect the ionization state and hydrophilic/hydrophobic balance in these hydrogels, shifting the LCT above or below ambient temperature.<sup>16</sup> Also, ionized monomer units and their counterions engender an osmotic pressure that affects swelling equilibrium.<sup>17</sup>

A major limitation of hydrogels lies in their tendency to fracture at small strains. Fracture arises from permanent inhomogeneities that are frozen in during network formation. Promising approaches to improve mechanical robustness of hydrogels include introduction

Correspondence to: Ronald A. Siegel (siege017@umn.edu).

of slipping crosslinks,<sup>18,19</sup> or a introducing a secondary network whose chains rapidly flow and relieve stresses at fracture initiation points in the primary network.<sup>18–21</sup> In a third approach introduced by Haraguchi and coworkers,<sup>22,23</sup> exfoliated Laponite nanoclay (NC) platelets are suspended in monomer solutions with initiator, followed by polymerization. Polymer chains form bridges between the platelets, and also entangle, thus forming a network. Such NC gels are easy to synthesize, and they exhibit excellent mechanical, optical and swelling properties.<sup>22,23</sup>

Most research on NC gels has been restricted to systems based on water soluble, thermosensitive neutral monomers such as NIPA and *N,N'*-dimethylacrylamide (DMAm).<sup>5,22,24–35</sup> In this paper we report the first synthesis of NC copolymer hydrogels based on *N*-isopropylacrylamide and ionizable comonomers. Weakly acidic and basic hydrogels have been produced, exhibiting complementary pH-sensitivities at physiological temperature (37 °C). We explore the swelling and mechanical behaviors of these hydrogels and demonstrate their robustness to large mechanical deformations. We also investigate effects of monomer composition on the process of gelation, using optical techniques. These hydrogels are promising as materials with tunable hydrophobicity and ionization states, for use as drug delivery systems and novel tissue culture substrates.<sup>5</sup>

## EXPERIMENTAL

### Materials

*N*-isopropylacrylamide (NIPA, monomer; Polysciences) was recrystallized from hexane/toluene and vacuum dried. Dimethylaminoethyl methacrylate (DMAEMA, monomer: Sigma-Aldrich) and methyl methacrylate (MMA, monomer: Sigma-Aldrich) were purified by passing through activated alumina (Sigma-Aldrich). Laponite XLG<sup>R</sup> (XLG: Rockwood Ltd.), an inorganic hectorite (Na<sub>0.66</sub>: cation exchange capacity 104meq/100g), sodium methacrylate (MAANa: Sigma Aldrich), *N,N'*-methylenebisacrylamide (Sigma Aldrich), potassium persulfate (KPS, initiator: Sigma-Aldrich), sodium pyrophosphate decahydrate (SPP, ionic dispersant: Sigma-Aldrich) and *N,N,N',N'*-tetramethylethylenediamine (TEMED, accelerator: Sigma-Aldrich) were used as received. Deionized water was used in all experiments. Acetate (pH=4–5.5), 2-(*N*-morpholino) ethane sulfonic acid (pH=5.5–6.5), and phosphate (pH=6.5–8.0) buffers were formulated at 20 mM, with NaCl added to set ionic strength at 155 mM.

### Copolymerization of NIPA with neutral and ionizable comonomers

Four types of copolymer gel were synthesized: 1) cationic copolymer hydrogels based on NIPA and DMAEMA; 2) anionic copolymer hydrogels based on NIPA and MAANa; 3) anionic hydrogels formed by copolymerizing NIPA and MMA and hydrolyzing MMA units to MAANa; and 4) anionic copolymer gels formed by polymerizing NIPA and MAA in the presence of SPP. NC hydrogels are designated as NX-mR, where “R” signifies the comonomer substituted for NIPA and “m” indicates the mol% substitution of that comonomer. Hydrolyzed MMA gels are labeled NX-mhMMA.

Hydrogels were obtained by redox-initiated free radical polymerization in water at 25 °C for 24 hours. Prepolymer solution compositions are given in Table 1. Synthesis procedures were similar for all hydrogels, with exceptions noted below. As a typical example, NX-10MMA hydrogel was synthesized with 1.2 g NIPA dissolved in 12.83 mL water. Next, XLG (0.53 g) was added under vigorous stirring, obtaining a stable dispersion (NIPA/XLG sol) after a few minutes. MMA (125.1 μL) was added dropwise into the dispersion, followed by vortexing for 2–3 minutes. Polymerization was initiated by spiking 675 μL of 20 mg/mL KPS and 30 μL TEMED into the dispersion.

Special considerations were: 1) A relatively high water content was required to synthesize NX-MAANa hydrogels without interruption by flocculation. In this case, 20 mg/mL aqueous solution of MAANa was added dropwise to the stable, pre-mixed NIPA/XLG sol (Table 1); 2) For NX-MAA hydrogels, SPP was added to the monomer solution before dropwise addition of MAA in order to prevent flocculation of the clay particles; 3) For organically crosslinked hydrogels, Laponite XLG was replaced by 0.11g (0.7 mmol) N,N'-methylenebisacrylamide.

For hydrolysis and swelling studies, hydrogels were cast between parafilm-covered glass plates separated by 0.8 mm teflon spacers, and were cut into ~11mm diameter disks using a cork borer. Parafilm eased separation of the NC hydrogels from the glass plates. Hydrogels were washed for ~2d to remove unreacted components and the sol fraction.

For tensile studies, hydrogels were cast in cylindrical glass tubes of 5.25 mm ID and 75 mm length, wrapped in parafilm, and stored for up to two weeks. No washing steps were performed.

### Equilibrium swelling

In the pH-dependent equilibrium swelling studies, hydrogel disks were equilibrated in different pH-buffers at 37 °C over two days, after which disk diameters were determined by light microscopy. The linear swelling ratio was calculated as  $LSR = [\text{diameter at equilibrium (mm)}] / (11 \text{ mm})$ . Swelling measurements were performed in duplicate and are reported with error bars representing standard deviations.

### Hydrolysis of NX-mMMA

To produce NX-mhMMA hydrogels, NX-mMMA disks were hydrolyzed in 0.1 N NaOH at 25 °C over selected periods, and washed thoroughly (~2d) in deionized water. Hydrolyzed samples were then equilibrated either in acidic (pH 4.5) or neutral (pH 7.4) nonhydrolyzing buffer for two days at 37 °C. Relative linear swelling ratios were calculated as  $RLSR = LSR(\text{pH } 7.4) / LSR(\text{pH } 4.6)$ . Hydrogels that had undergone 5 d hydrolysis were subjected to pH-sensitive swelling protocols, as above.

### Mechanical properties

Ultimate tensile properties of cylindrical hydrogels were measured in a tensile tester (MTS QTest Tensile Testing Machine). Just before testing, the tubes containing the hydrogels were carefully broken and the hydrogels were removed. The two tips of the hydrogels were wrapped in sandpaper (213Q Imperial Wet or Dry sheet, 3M) to prevent slippage, and clamped into the tensile tester. Tensile measurements were performed at 25 °C with gauge length 15 mm and crosshead speed 100 mm/min. Elongation strain at break,  $\epsilon_b$ , stress at break,  $\sigma_b$ , and average tensile moduli  $E_{10-50}$  and  $E_{100-200}$  over the 10–50% and 100–200% strain ranges, respectively, were recorded for each hydrogel. Tensile testing results were verified by duplication.

### Transparency changes during polymerization

Transparency changes during polymerization were measured in a UV/vis spectrophotometer (Cary 100). After mixing all the components, the pregel solution was poured into a cuvette (10×4×45 mm, Sarstedt), capped, and placed in the sample holder. Percent transmittance at 600 nm during polymerization was monitored for 200 minutes.

## RESULTS

### Synthesis and pH-dependent swelling

**DM-DM polybase hydrogels**—The NIPA/clay sol was stable with up to 0.2 mM DMAEMA added. Following initiation by KPS/TEMED, polymerization proceeded similarly to NC gels based on NIPA and DMAm homopolymers.<sup>21·26·30</sup>

Results of equilibrium swelling studies carried out on the NX-DM hydrogels at 37 °C, as a function of pH, are displayed in Figure 1. pH-sensitivity was not observed at low DMAEMA substitutions (NX-2DM and NX-5DM gels). With greater than 5 mol% substitution, however, a significant swelling transition was observed, with hydrogels swelling at lower pH values and shrinking at higher pH, as expected from the basic character of DMAEMA. The NX-10DM hydrogel exhibited a sharp swelling transition near pH 8, while NX-20DM hydrogel's transition was broader and was shifted towards the more alkaline range, pH~8.7–8.9. The NX-20DM hydrogels, with higher DMAEMA content, swelled more than the NX-10DM hydrogels.

**NX-MAANa polyacid hydrogels**—The first approach to introduce weak acid MAA comonomers without flocculating the NIPA/XLG sol was to increase the sol's water content, followed by drop-wise addition of MAANa salt solution. By this approach, up to 10 mol% comonomer with respect to NIPA could be introduced and polymerized to form NX-MAANa hydrogels. While the relative concentration of Laponite XLG with respect to the monomers did not change when water was added, absolute XLG concentration was decreased, and the hydrogels were dilute and comparatively weak.

As illustrated Figure 2, the NX-MAANa hydrogels underwent a transition from a relatively collapsed state at low pH to a swollen state at high pH. With increasing acid comonomer content in the hydrogel, the transition was magnified and an acid shift in transition pH was observed. Gels consisting of NX-10MAANa exhibited a swelling transition near the pKa of MAA (pKa=4.7) whereas for NX-3MAANa, the swelling transition was observed around pH=5.5. A small swelling transition was observed for NX-2MAANa near pH=6.8.

**NX-hMMA polyacid hydrogels**—In the second approach to introduce acid groups into NC hydrogels, preformed NX-MMA was hydrolyzed in strong base (0.1N NaOH) to convert pendant MMA groups into MAANa sidegroups. Although MMA is sparingly soluble in water, there was no trouble adding required amounts of MMA to the NIPA/XLG sol. We were able to synthesize NX-MAA hydrogels with up to 20 mol% MMA in the copolymer feed, beyond which clay flocculation interfered.

Alkaline hydrolysis of NX-MMA hydrogels was monitored by stopping hydrolysis at specified times, and comparing equilibrium swelling values for gels re-equilibrated in low pH (4.5) and high pH (7.4) buffers at 37 °C. Results, expressed as relative linear swelling ratios (RLSR's) are shown in Figure 3. While only slight relative swelling was observed at pH 4.5 after Day 1, swelling at pH 7.4 increased steadily until Day 5, indicating progressive hydrolysis of MMA sidechains to MAA pendant groups.

Equilibrium swelling studies carried out on NX-hMMA hydrogels, following five days of hydrolysis, were carried out as a function of pH, and are summarized using LSR's in Figure 4. NX-10hMMA and NX-20hMMA hydrogels exhibited a significant swelling transition between pH 5 and 6. The swelling response was slightly less for NX-20hMMA than for NX-10hMMA, and the transition was shifted in the alkaline direction for NX-20hMMA. Swelling of the hydrolyzed systems was not as significant as it was for NX-MAANa hydrogels of similar composition, probably due to incomplete hydrolysis.

NX-hNIPA hydrogels displayed a comparatively weak swelling dependence on pH (Figs. 3 and 4), perhaps due to anionic charges on the clay surfaces, or to a dilute fraction of hydrolyzed NIPA sidechains.

**NX-MAA polyacid hydrogels**—In the most successful approach to incorporate MAA groups into the NC hydrogels, SPP was added to NIPA/XLG sol before introducing neutral MAA. With proper amounts of SPP, depending on MAA content (Table 1), clay flocculation was prevented and strong, transparent NX-MAA hydrogels were obtained with up to 10 mol % MAA in the reaction feed. At a given MAA content, the amount of SPP that could be added was bounded below by flocculation, and above by formation of turbid gels.

Equilibrium swelling of NX-MAA hydrogels at 37 °C as a function of pH, is reported in Figure 5. All NX-MAA hydrogels exhibited a sharp volume transition over narrow pH ranges. Generally, swelling of NX-MAA hydrogels was much greater than for NX-hMMA hydrogels, and slightly exceeded or was comparable to swelling of NX-MAANa hydrogels containing equivalent amounts of acid groups. As with NX-MAANa hydrogels, the degree of swelling increased and the volume transition pH underwent an acid shift with decreasing mol% MAA.

### Mechanical properties

Tensile tests were carried out in cylindrical gels that had not yet been exposed to swelling media, since swollen hydrogels were too slippery. It was not possible to estimate the mechanical properties of the hydrolyzed NX-hMMA hydrogels directly since the latter swelled significantly during hydrolysis, and we report the tensile properties of the unhydrolyzed NX-MMA hydrogels.

Results are summarized in Table 2. All NC hydrogels except the NX-MAANa compositions were highly elastic and exhibited elongation strains at break ( $\epsilon_b$ ) in the range 600–1000% (Table 2). NX-MAANa hydrogels with 2–5% MAANa could be elongated to a lesser degree, while the NX-10MAANa were slippery and fractured during sample loading. Organic (bisacrylamide) crosslinked hydrogels with otherwise similar comonomer content to the NC hydrogels were extremely fragile, and also fractured during sample loading onto the tensile tester. The generally excellent tensile properties of the NC hydrogels can be attributed to the nanoclay crosslinkers, consistent with previous reports for homopolymeric NC hydrogels.<sup>30,31</sup>

An overall but not totally consistent trend was for  $\epsilon_b$  to decrease with increasing comonomer substitution. Related trends were observed for break stress,  $\sigma_b$ , and the intermediate elongational moduli,  $E_{10-50}$  and  $E_{100-200}$ . In most cases, small amounts of comonomer increased  $\sigma_b$ ,  $E_{10-50}$  and  $E_{100-200}$ , compared to values observed in NX-100N (NIPA homopolymer) hydrogel, but further increases in substitution led to decreasing values of these characteristics.

### Optical Transparency Changes during Polymerization

Figure 6 reports time-dependent changes in optical transmittance recorded during room temperature polymerization of NX gels. These results are similar to those previously reported with nanocomposite hydrogels based on poly(*N*-isopropylacrylamide).<sup>27,36</sup> The NX-MAANa hydrogels were an exception, however, exhibiting only a small change in transparency during polymerization. Both NX-5MAANa and NX-10MAANa hydrogels were very cloudy (~15–30% transmittance) even before polymerization was initiated (Figure 6b), probably due to flocculated aggregates of laponite particles in the monomer solution.



At the start of polymerization, all other monomer/clay solutions exhibited high transparency (80–90%). Transmittance remained constant for some time after initiator was added, and then decreased sharply over a few minutes, reaching a minimum and finally recovering back to a steady level. Transmittance changes for NX-100NIPA were consistent with earlier reports.<sup>27,36,37</sup> Induction time decreased with increasing mol% of MAA, MMA or DMAEMA in the monomer solution. Low to moderate transmittance recoveries were observed for all NX hydrogels. However, NX-100NIPA hydrogels demonstrated complete recovery of its original transparency.

## DISCUSSION

Laponite XLG consists of layered silicate nanodiscs with negatively charged faces and slightly positively charged edges. The net cation exchange capacity is 104 meq/100g of clay. A house-of-cards structure forms in moderately concentrated clay solutions due to attractive interactions between oppositely charged surfaces and edges, resulting in flocculation or “gelling.”<sup>38–40</sup> Flocculation can be inhibited by nonionic monomers such as NIPA and DMAEM, which form hydrogen bonds with the clay surface, shielding the charged clay particles from each other and stabilizing the dispersion.<sup>26,27,35</sup>

A three-step mechanism has been proposed for formation of NC hydrogel networks.<sup>27</sup> Initially, a stable aqueous dispersion consisting of exfoliated Laponite platelets is formed in aqueous prepolymer solution. Initiator and accelerator species adsorb on the clay edges and initiate polymerization. As the polymer chains grow, a stable three dimensional polymer/clay network is established through hydrogen bonding between the poly(NIPA) chains and the exfoliated clay surfaces. The first step is considered the most critical, as addition of monomer, initiator and accelerator must not disturb the dispersion’s colloidal stability.<sup>41</sup> Salts, ionic monomers, and miscible solvents such as methanol weaken electrical double layer repulsive forces between clay platelets, and van der Waals forces trigger flocculation.<sup>42</sup> For this reason, it has been difficult to synthesize hydrogels beyond those based on neutral *N*-substituted alkylacrylamides in 100% aqueous systems.

Recently, Song et al.<sup>41</sup> synthesized a double network hydrogel system with poly(acrylic acid) chains interpenetrating a NC poly(NIPA) hydrogel. The pH response of these hydrogels was attenuated compared to conventionally crosslinked NIPA/acrylic acid or NIPA/methacrylic acid hydrogels.<sup>43</sup> Also, optical clarity of the double network hydrogels was significantly compromised compared to the NC hydrogels synthesized with NIPA alone.

The theme of the present paper was to find methods to avert the clay flocculation problem, and to synthesize single network NC hydrogels exhibiting improved pH-sensitivity at 37 °C and robust mechanical properties. We first comment on the individual formulations, one for polybase hydrogels and three for polyacid hydrogels. We then turn to general discussions of tensile phenomena, and of optical properties during synthesis.

### NX-DM polybase hydrogels

Mechanically robust NX-DM hydrogels were formed with up to 20 mol% DMAEMA substitution in the usual NIPA/clay sol. Apparently, the basic DMAEMA monomer did not disrupt colloidal stability of the NIPA/XLG sol, perhaps because the monomer’s weak positive charge inhibited formation of the house of cards.

The  $pK_a$  of DMAEMA is close to 8, so the pH-sensitivity observed for NX-10DM and NX-20DM hydrogels (Figure 1) is consistent with expectation. With increasing DMAEMA content, the net ionization of NX-DM at any given pH also increases, allowing osmotic

swelling forces to overcome hydrophobicity, which is conferred primarily by NIPA at 37 °C. This simple consideration explains both the alkaline shift of volume transition pH and the increased degree of swelling over the volume transition with increasing mol% DMAEMA.<sup>44</sup>

The absence of pH-sensitivity for hydrogels with <10% DMAEMA might result from strong binding of tertiary amine molecules to the negatively charged surfaces of the clay particles. These bound amine molecules may have been unable to contribute to pH-sensitivity in the hydrogel.

### **NX-MAANa polyacid hydrogels**

Copolymerization of NIPA and MAANa in diluted NIPA/clay sol reduced or slowed but probably did not completely eliminate clay flocculation when MAANa was added, as evidenced by the translucence of the clay sols. The resulting hydrogels were dilute polymer networks with low crosslink densities and relatively weak mechanical properties. (We speculate that the efficacy of this technique might degrade further if the diluted clay/NIPA sol is stored, and more time is permitted for flocculation.) However, NX-MAANa hydrogels were stronger than their organically crosslinked counterparts, which invariably failed during sample loading.

With increased MAA substitution, swelling increased at any given pH, and the swelling transition point shifted in the acid direction. This shift was opposite to the base shift in transition seen with increasing DMAEMA incorporation in the polybase hydrogels, but the explanation is the same: increased content of ionizable groups requires that a smaller fraction of these groups be ionized to overcome network hydrophobicity.

### **NX-hMMA Polyacid Hydrogels**

We were unable to measure the tensile properties of the hydrolyzed NX-hMMA hydrogels since they were swollen and slippery, so we focus here on the unhydrolyzed NX-MMA hydrogels. These materials exhibited higher  $\sigma_b$  values than NX-NIPA hydrogels, at the expense of a small reduction in  $\epsilon_b$ . These trends may be due to enhanced hydrophobic interactions between neighboring polymer chains in NX-MMA hydrogels. Similar differences have been reported in tensile properties of Laponite crosslinked hydrogels where the only differences between the two homopolymers, poly(NIPA) and the more hydrophilic poly(N,N-dimethylacrylamide) were the flexibility and hydrophilicity of the polymer chains.<sup>22</sup>

Swelling of hydrolyzed NX-hMMA hydrogels was reduced compared to the NX-MAANa hydrogels, probably due to incomplete hydrolysis of MMA groups, even after days of exposure to strong base. It is also noteworthy that NX-20hMMA hydrogels with 20 mol% initial MMA substitution swelled less than NX-10hMMA hydrogels, and that increased substitution lead to an alkaline shift in swelling transition, opposite to that seen with the NX-MAANa hydrogels. Increased incorporation of MMA increases chain hydrophobicity and interchain association, potentially shielding MMA groups from the alkaline pH environment during the hydrolysis step and reducing conversion to MAA. Also, the presence of unhydrolyzed MMA in the network increases that latter's hydrophobicity, leading to a higher degree of dissociation of ionizable groups needed for the swelling transition, hence the alkaline shift in swelling behavior.

### **NX-MAA Polyacid Hydrogels**

Addition of pyrophosphate (SPP) ions were added to the clay sol before MAA produced anionic hydrogels that combined the superior pH-responsiveness of NX-MAANa hydrogels

with the robust tensile properties of NX-MMA hydrogels. The pyrophosphate ions stabilized the aqueous nanoclay dispersion, presumably by binding to the charged rims of the exfoliated nanoclay platelets and inhibiting house of cards association and flocculation of the clay particles, as reported previously.<sup>45</sup> The dispersing behavior of pyrophosphate ions is opposite to the aggregation tendency of monovalent salts, probably due to a charge inversion effect that is known to occur when multivalent ions are added to colloidal dispersions.<sup>46,47</sup>

Recently, Negrete-Herrera et al.<sup>48</sup> utilized pyrophosphate anions to redisperse flocculated Laponite clay particles used in Pickering emulsion polymerization of poly(styrene-co-butylacrylate). Liu et al.<sup>49,50</sup> produced low viscosity, high concentration Laponite dispersions in water using a “sol-grade” Laponite XLS instead of the “gel-grade” Laponite XLG used in Haraguchi’s work.<sup>22,26,30,31</sup> These stable dispersions were subsequently employed to synthesize *N*-isopropylacrylamide based hydrogels with exceptionally high tensile strength. The main difference between the two grades of clay particles was the modification of positively charged rims of the clay platelets with small quantities of SPP (~ 8.35% w/w to clay) in Laponite XLS.

Using SPP during the polymerization step eliminated the need for special sol-grade Laponite (XLS). The amount of SPP, up to 50% w/w (to clay) required to arrest flocculation during synthesis of NX-MAA hydrogels with XLG greatly exceeded the amount present in XLS. The reason for this difference is unclear at this stage. Depending upon the mol% acid in the copolymer hydrogel feed, the amount of SPP used was optimized to obtain NX-MAA hydrogels with very high optical transparency. Higher amounts of SPP were required as the mol% MAA in the recipe increased.

NX-MAA hydrogels exhibited the highest pH-sensitivity among all the anionic hydrogels (Figure 5). This behavior may also be due to the pyrophosphate modification and charge inversion occurring on the rims of the clay particles. With the clay particles negatively charged around their whole surface, the Donnan ionic osmotic pressure should increase,<sup>51,52</sup> and surface/edge attractions should be eliminated.

Swelling transitions shifted in the acid direction with increasing MAA substitution in the NX-MAA hydrogels. As with the NX-MAANa hydrogels, this trend is explained by the increased availability of ionizable groups, and a smaller fraction of those groups required to overcome the hydrophobic effects due primarily to NIPA.

### Tensile properties

With the exception of the NX-10hMAANa composition, the NC polyelectrolyte hydrogels exhibited extensibilities ( $\epsilon_b$ ) that are far superior to corresponding conventional hydrogels made with organic crosslinkers, and within the same ballpark as uncharged homopolymer hydrogels that were studied previously. The reader is reminded that all tensile measurements were made in the hydrogels’ formation state, rather than after equilibrium swelling. This choice was necessitated by the chosen tensile testing method, and is in line with previously published literature. It will be fruitful in the future to address the effect of pH-dependent swelling on the mechanical properties of these hydrogels. Methods involving alternative hydrogel geometries or compression testing should be contemplated.

A common trend for all the formulations was that tensile strength at break ( $\sigma_b$ ) was enhanced with low substitution of guest (non-NIPA) comonomer, relative to homo-NIPA hydrogels. With increasing substitution, however,  $\sigma_b$  declined. Full explanation of origins of this trend may be premature, and the mechanisms may be formulation specific. We speculate, however, that the behavior may be due to effects of comonomer concentrations on



clay exfoliation and aggregation. More extensive data and investigations of evolving sol structure may shed further light on this issue. Similar comments apply to the intermediate moduli,  $E_{10-50}$  and  $E_{100-200}$ .

### Transmittance changes during polymerization

Transparency changes during polymerization of nanocomposite hydrogels have been reported earlier with Laponite crosslinked poly(N-isopropylacrylamide).<sup>27,36,37</sup> These changes were not observed during polymerization with organic crosslinkers. Loss of transparency during the early stages of polymerization probably occurs due to formation of small polymer brushes on the nanoclay particle surfaces, with dimensions on the order of the wavelength of visible light. Recovery of transparency eventually occurs as polymer chains fill the volume and network formation takes place. In the present studies, the recovery phase was always followed (even in NX-100NIPA hydrogels) by a slow reduction in light transmission, which may reflect long term relaxations in hydrogel structure.

Except for the NX-MAANa hydrogels, transmittance loss followed by recovery was observed in all NX hydrogels (Figure 6a–d). Near complete recovery of transmittance was observed only with NX-100NIPA hydrogels. As overall copolymer hydrophobicity increased, the percent recovery in transmittance decreased. This effect was consistently observed in the polybasic NX-DM, neutral NX-MMA and anionic NX-MAA hydrogels. Optical changes observed in NX-MAANa hydrogels during polymerization were not as remarkable. The reduced recovery observed for NX-DM, NX-MMA and NX-MAA hydrogels may reflect aggregation between nearby polymer chains through various weak intermolecular interactions such as hydrogen bonding. With increasing network hydrophobicity the time to attain the minimum in transmittance was reduced. Accelerated development of turbidity could be due to faster copolymerization kinetics of NIPA with more hydrophobic comonomers, or more rapid formation of sub-micron sized polymer-clay brushes and aggregates of these nanostructures.

## CONCLUSIONS

pH and temperature sensitive nanoclay composite hydrogels with excellent mechanical properties have been reported for the first time. Straightforward synthetic schemes that overcame the tendency of clay to flocculate, were adopted in preparing these hydrogels. Cationic comonomers such as amine containing acrylates could be easily copolymerized with NIPA and incorporated into the hydrogel matrix to produce polybasic hydrogels exhibiting pH-dependent swelling at 37 °C. Anionic comonomers based on acrylic acid derivatives were slightly more difficult to incorporate due to the tendency of the nanoclay particles to coagulate. Three strategies were employed to overcome this problem. Of the three, pretreatment with pyrophosphate ions was found to be the most successful in producing highly pH-sensitive hydrogels at 37 °C with excellent tensile characteristics. pH-sensitivity in the hydrogel could be easily tuned by adjusting acid or base comonomer content. The availability of strong pH-sensitive hydrogels is expected to extend the utility of hydrogels in various applications such as drug delivery.

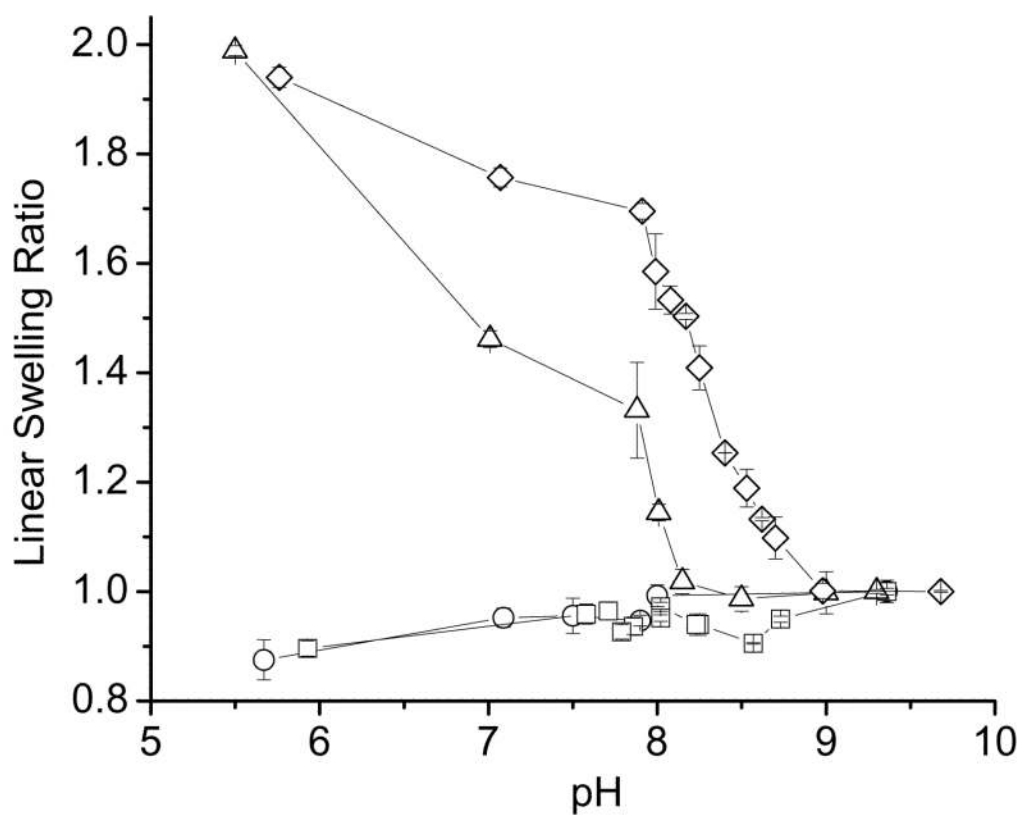
## Acknowledgments

We thank Prof. Chun Wang (Biomedical Engineering, University of Minnesota) and Zhongli Dai for their help in the use of the MTS Tensile Testing equipment. We also thank Prof. Chris Macosko and Dr. Mike Dolgovskij for providing us with sample of Laponite XLG.

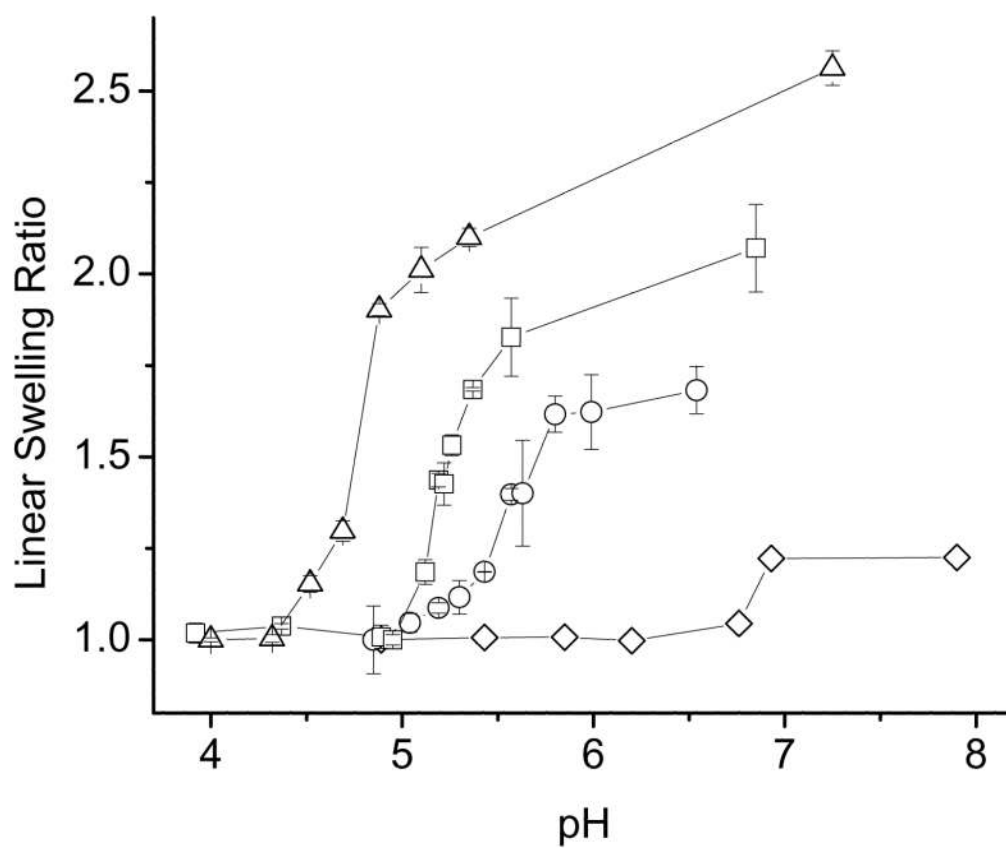
## References

1. Jeong SH, Huh KM, Park K. *Polymers in Drug Delivery*. 2006;49–62.
2. Kikuchi A, Okano T. *Adv Drug Deliver Rev*. 2002; 54:53–77.
3. Peppas NA, Bures P, Leobandung W, Ichikawa H. *Eur J Pharm Biopharm*. 2000; 50:27–46. [PubMed: 10840191]
4. Stile RA, Healy KE. *Biomacromolecules*. 2001; 2:185–194. [PubMed: 11749171]
5. Haraguchi K, Takehisa T, Ebato M. *Biomacromolecules*. 2006; 7:3267–3275. [PubMed: 17096560]
6. Tessmar JK, Goepferich AM. *Macromol Biosci*. 2007; 7:23–39. [PubMed: 17195277]
7. Baldi A, Lei M, Gu Y, Siegel RA, Ziaie B. *Sensor Actuat B-Chem*. 2006; B114:9–18.
8. Lei M, Gu Y, Baldi A, Siegel RA, Ziaie B. *Langmuir*. 2004; 20:8947–8951. [PubMed: 15461469]
9. Ohashi H, Hiraoka Y, Yamaguchi T. *Macromolecules*. 2006; 39:2614–2620.
10. Okajima S, Sakai Y, Yamaguchi T. *Langmuir*. 2005; 21:4043–4049. [PubMed: 15835972]
11. Chun SW, Kim JD. *J Control Release*. 1996; 38:39–47.
12. Peppas N, Khare AR. *Adv Drug Deliver Rev*. 1993; 11:1–35.
13. Shiotani A, Mori T, Niidome T, Niidome Y, Katayama Y. *Langmuir*. 2007; 23:4012–4018. [PubMed: 17311430]
14. Kudaibergenov S, Jaeger W, Laschewsky A. *Adv Polym Sci*. 2006; 201:157–224.
15. Qiu Y, Park K. *Adv Drug Deliver Rev*. 2001; 53:321–339.
16. Kawasaki H, Sasaki S, Maeda H. *J Phys Chem B*. 1997; 101:5089–5093.
17. Hirotsu S, Hirokawa Y, Tanaka T. *J Chem Phys*. 1987; 87:1392–1395.
18. Okumura Y, Ito K. *Adv Mater*. 2001; 13:485–487.
19. Tanaka Y, Gong JP, Osada Y. *Prog Polym Sci*. 2005; 30:1–9.
20. Gong JP, Katsuyama Y, Kurokawa T, Osada Y. *Adv Mater*. 2003; 15:1155–1158.
21. Bishop M, Shahid N, Yang J, Barron AR. *Dalton T*. 2004:2621–2634.
22. Haraguchi K, Farnworth R, Ohbayashi A, Takehisa T. *Macromolecules*. 2003; 36:5732–5741.
23. Haraguchi K, Takehisa T. *Adv Mater*. 2002; 14:1120–1124.
24. Haraguchi K, Ebato M, Takehisa T. *Adv Mater*. 2006; 18:2250–2254.
25. Haraguchi K, Li HJ. *Angew Chem Int Ed*. 2005; 44:6500–6504.
26. Haraguchi K, Li HJ. *Macromolecules*. 2006; 39:1898–1905.
27. Haraguchi K, Li HJ, Matsuda K, Takehisa T, Elliott E. *Macromolecules*. 2005; 38:3482–3490.
28. Haraguchi K, Matsuda K. *Chem Mater*. 2005; 17:931–934.
29. Haraguchi K, Takada T. *Macromol Chem Phys*. 2005; 206:1530–1540.
30. Haraguchi K, Takehisa T. *Adv Mater*. 2002; 14:1120–1124.
31. Haraguchi K, Takehisa T, Fan S. *Macromolecules*. 2002; 35:10162–10171.
32. Haraguchi K, Taniguchi S, Takehisa T. *ChemPhysChem*. 2005; 6:238–241. [PubMed: 15751345]
33. Guo X, Li L, Prud'homme RK. *PMSE Preprints*. 2006; 94:59–60.
34. Shibayama M, Karino T, Miyazaki S, Okabe S, Takehisa T, Haraguchi K. *Macromolecules*. 2005; 38:10772–10781.
35. Shibayama M, Suda J, Karino T, Okabe S, Takehisa T, Haraguchi K. *Macromolecules*. 2004; 37:9606–9612.
36. Zhu M, Liu Y, Sun B, Zhang W, Liu X, Yu H, Zhang Y, Kuckling D, Adler HJP. *Macromol Rapid Commun*. 2006; 27:1023–1028.
37. Miyazaki S, Endo H, Karino T, Haraguchi K, Shibayama M. *Macromolecules*. 2007; 40:4287–4295.
38. Bonn D, Kellay H, Tanaka H, Wegdam G, Meunier J. *Langmuir*. 1999; 15:7534–7536.
39. Mouchid A, Lecolier E, Van Damme H, Levitz P. *Langmuir*. 1998; 14:4718–4723.
40. Fossum JO. *Physica A*. 1999; 270:270–277.
41. Song L, Haraguchi K. *Kawamura Rikagaku Kenkyusho Hokoku*. 2006:19–25.

42. Olphen, HV. An introduction to clay colloid chemistry: for clay technologists, geologists, and soil scientists. Wiley; New York: 1977.
43. Mujumdar SK, Bhalla AS, Siegel RA. *Macromol Symp.* 2007; 254:338–344.
44. Siegel RA, Firestone B. *Macromolecules.* 1988; 21:3254–3259.
45. Mongondry P, Nicolai T, Tassin JF. *J Colloid Interf Sci.* 2004; 275:191–196.
46. Nguyen TT, Grosberg AY, Shklovskii BI. *J Chem Phys.* 2000; 113:1110–1125.
47. Nguyen TT, Grosberg AY, Shklovskii BI. *Phy Rev Lett.* 2000; 85:1568–1571.
48. Negrete-Herrera N, Putaux JL, David L, Bourgeat-Lami E. *Macromolecules.* 2006; 39:9177–9184.
49. Liu Y, Zhu M, Liu X, Zhang W, Sun B, Chen Y, Adler H-JP. *Polymer.* 2006; 47:1–5.
50. Zhang W, Liu Y, Zhu M, Zhang Y, Liu X, Yu H, Jiang Y, Chen Y, Kuckling D, Adler H-JPJ. *Polym Sci A.* 2006; 44:6640–6645.
51. Flory PJ, Rehner JJ. *J Chem Phys.* 1943; 11:512.
52. Flory PJ, Rehner JJ. *J Chem Phys.* 1943; 11:521.

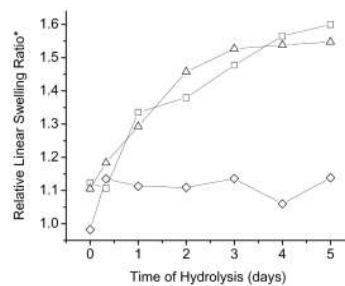


**Figure 1.** pH-dependent equilibrium swelling studies at 37 °C for NX-DM gels. All buffered solutions had an ionic strength of 155 mM. (○) NX-2DM; (□) NX-5DM; (△) NX-10DM; (◇) NX-20DM. In this and in subsequent figures, linear swelling ratio can be converted to volume swelling ratio by cubing.

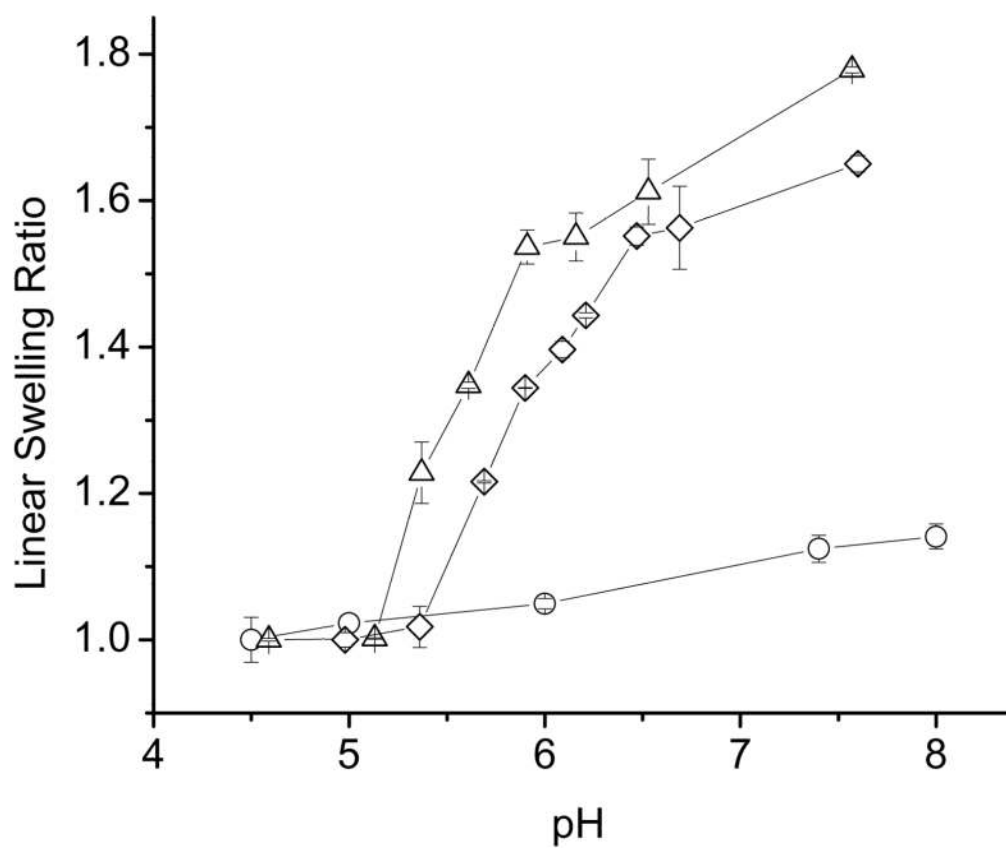


**Figure 2.** pH-dependent equilibrium swelling studies at 37 °C for NX-MAANa gels. (◇) NX-2MAANa; (○) NX-3MAANa; (□) NX-5MAANa; (△) NX-10MAANa.

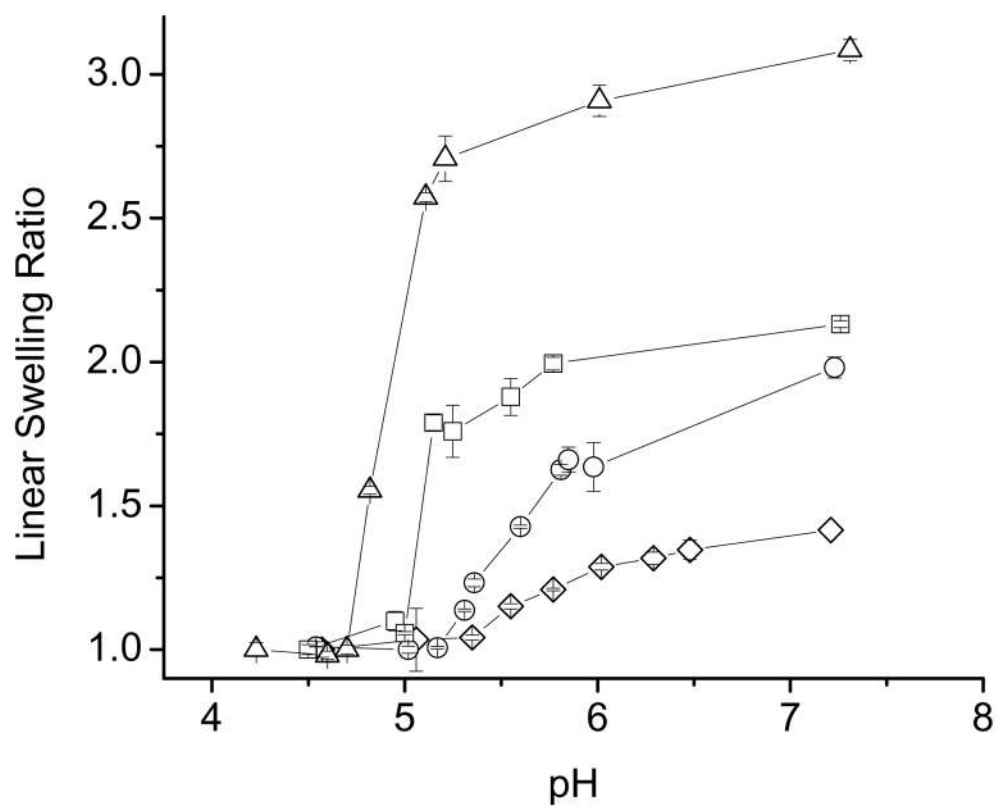




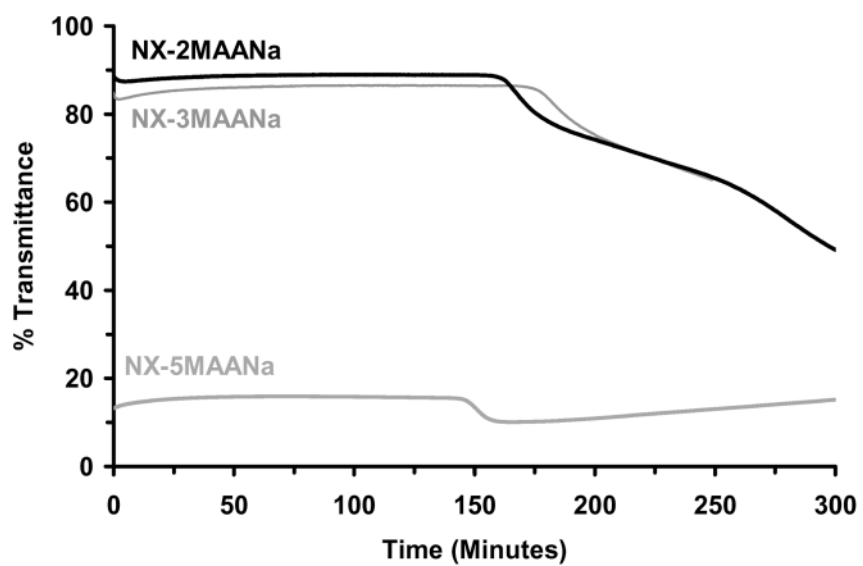
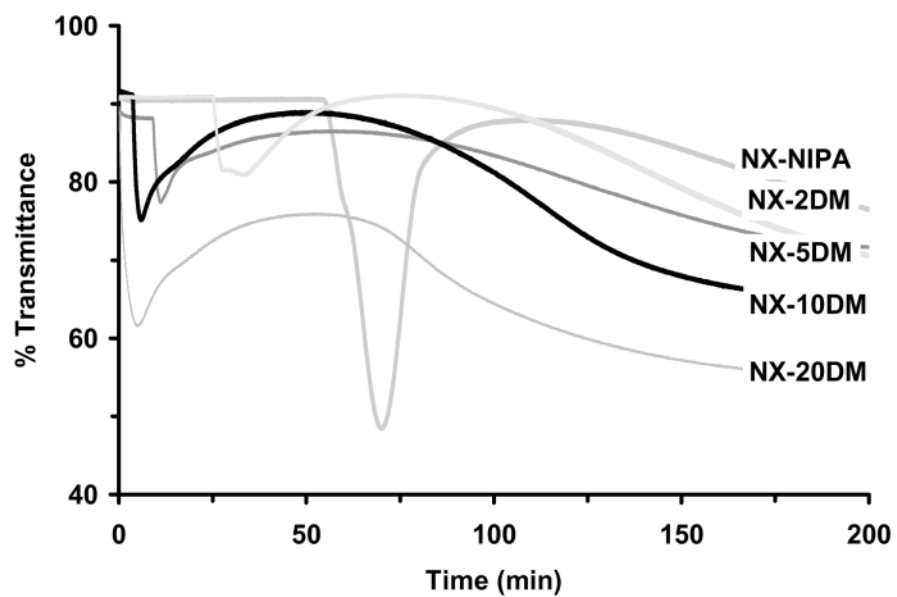
**Figure 3.** Change in the linear swelling ratio of NX-MMA hydrogels as a function of the time of hydrolysis in 0.1 N NaOH. The Y-axis (Linear Swelling Ratio) is a ratio of the hydrogel diameter at pH 7.4 to its diameter at pH 4.5. (◇) NX-NIPA; (□) NX-10MMA; (△) NX-20MMA.



**Figure 4.** pH-dependent equilibrium swelling studies at 37 °C in NX-hMMA gels. (○) NX-hNIPA; (△) NX-10hMMA; (◇) NX-20MMA.



**Figure 5.** pH-dependent equilibrium swelling studies at 37 °C in NX-MAA gels. (◇) NX-2MAA; (○) NX-3MAA; (□) NX-5MAA; (△) NX-10MAA.



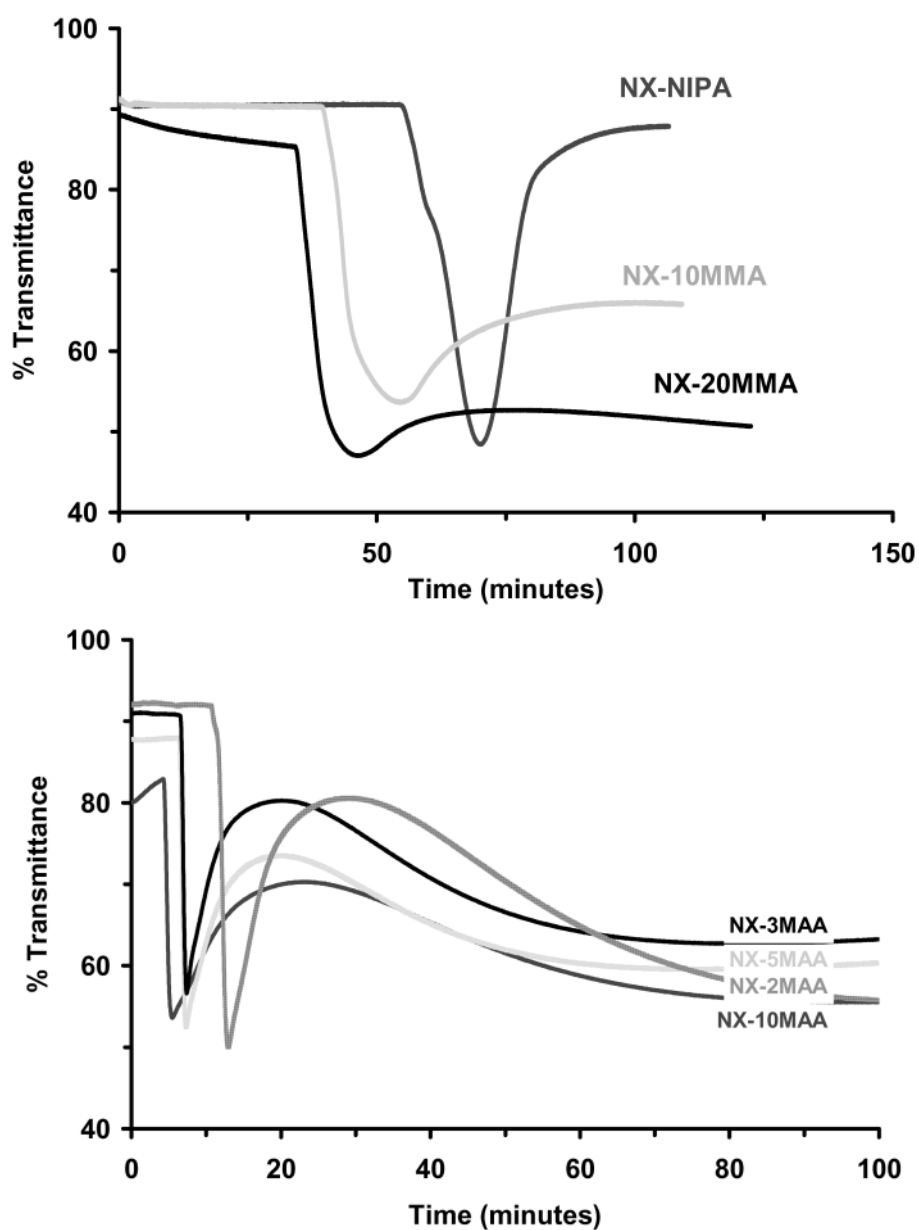


**Figure 6.** Change in the optical transmittance during polymerization. (a) NX-DM; (b) NX-MAANa; (c) NX-MMA; (d) NX-MAA.



Table 1

Feed compositions and tensile properties of NX gels based on NIPA and ionic comonomers.

Hydrogel	Composition <sup>a</sup>							
	NIPA g	DMAEMA $\mu$ L	MMA $\mu$ L	MAA <sup>a</sup> mL	MAA $\mu$ L	SPP g	H <sub>2</sub> O mL	
NX-100N	1.34	-	-	-	-	-	12.8	
NX-2DM	1.32	40.2	-	-	-	-	12.8	
NX-5DM	1.28	100.4	-	-	-	-	12.8	
NX-10DM	1.21	200.9	-	-	-	-	12.8	
NX-20DM	1.08	401.7	-	-	-	-	12.8	
NX-2MAA <sup>a</sup> Na	1.32	-	-	1.287	-	-	21.0	
NX-3MAA <sup>a</sup> Na	1.31	-	-	1.931	-	-	21.0	
NX-5MAA <sup>a</sup> Na	1.28	-	-	3.215	-	-	21.0	
NX-10MAA <sup>a</sup> Na	1.21	-	-	6.012	-	-	30.0	
NX-10MMA	1.21	-	125.1	-	-	-	12.8	
NX-20MMA	1.07	-	250.6	-	-	-	12.8	
NX-2MAA	1.32	-	-	-	20.2	0.090	12.8	
NX-3MAA	1.31	-	-	-	30.4	0.135	12.8	
NX-5MAA	1.28	-	-	-	50.5	0.113	12.8	
NX-10MAA	1.21	-	-	-	101	0.450	12.8	

<sup>a</sup> All recipes also include 675  $\mu$ L KPS solution (20 mg/mL), 30  $\mu$ L of TEMED and 0.53g of Laponite XLG.

<sup>b</sup> 20 mg/mL solution in H<sub>2</sub>O.

**Table 2**

Tensile properties of NX gels based on NIPA and ionic comonomers.

Hydrogel <sup>a</sup>	Stress at Break $\sigma_b$ (KPa)	Elongation at Break $\epsilon_b$ (%)	Tensile Modulus $E_{10-50}$ (KPa)	Tensile Modulus $E_{100-200}$ (KPa)
NX-100N	36.1	1010	10.7	9.60
NX-2DM	93.3	830	12.9	14.7
NX-5DM	79.3	736	28.8	12.6
NX-10DM	58.2	776	16.8	12.2
NX-20DM	40.4	858	14.5	5.26
NX-2MAANa	21.8	450	12.1	7.09
NX-3MAANa	19.6	377	12.5	6.15
NX-5MAANa	10.0	211	9.95	3.37
NX-10MAANa <sup>b</sup>	-	-	-	-
NX-10MMA	69.4	901	17.6	13.6
NX-20MMA	62.0	600	27.0	13.9
NX-2MAA	98.2	890	7.77	18.8
NX-3MAA	60.0	803	6.21	8.26
NX-5MAA	36.7	805	10.3	6.44
NX-10MAA	22.5	705	6.44	5.87

<sup>a</sup>Water contents of hydrogels are given in Table I.<sup>b</sup>These gels were extremely weak and ruptured during handling.